Integrated Non-Reciprocal Dual H- and E-Field Tunable Bandpass Filter with Ultra-Wideband Isolation

Hwaider Lin[1], Jing Wu[1], Xi Yang[2], Zhongqiang Hu[1], Tianxiang Nan[1], Satoru Emori[1], Yuan Gao[1], Rongdi Guo[1], Xinjun Wang[1], and Nian X. Sun[1]*

[1]Department of Electrical and Computer Engineering, Northeastern University, Boston, MA 02115 USA
[2]Beijing Institute of Technology, Beijing 100083, China
*Author currently works in Avago Technologies, San Jose, CA 95131 USA

Abstract — The integrated non-reciprocal tunable bandpass filter with a NiZn feritte film deposited via a spin sprayed process is presented. With external in-plane magnetic fields from 100 to 400Oe, the central frequency was tuned from 3.78 to 5.27GHz, with an insertion loss of 1.73 to 3.42dB and an in-band isolation of more than 13 dB, which was attributed to the non-reciprocity characteristics of the magnetostatic surface wave. By attaching the BPF on a PMN-PT slab, it can perform a voltage tunable behavior by magnetoelectric coupling. Frequency tunabilities of 500MHz/100Oe and 55MHz/1(kV/cm) are achieved. This design with dual functionality of integrated tunable bandpass filters and an UWB isolator can lead for compact, low-cost and power-efficient RF communication systems on RFIC and MMIC.

Index Terms —non-reciprocal, integrated, tunable bandpass filter, magnetostatic surface wave, ferrite, magnetoelectric

I. Introduction

Ultra-wideband (UWB) communication systems need reconfigurable subsystems such as tunable band-pass filters and isolators with a large bandwidth between the sensitive receiver and power transmitter. Non-reciprocal performance of magnetostatic surface wave (MSSW) in microwave ferrites, provide the possibility of realizing such a non-reciprocal device [1]-[3]. Recently, *Wu et al*. [4] demonstrated a non-reciprocal C-band magnetic tunable bandpass filter with ultra-wideband isolation by using a rotated YIG slab. He proposed a method by rotating the YIG slab by ~45° for suppressing reflection of MSSW modes at the slab edges. The central frequency was tuned from 5.2 to 7.5GHz, with an insertion loss of 1.6 to 3 dB and an isolation of more than 20dB.

Multiferroic composite materials with magnetoelectric (ME) coupling have led to tunable microwave magnetic devices such as resonators, phase shifters, etc. Most recently, people had demonstrated that by using a magnetoelectric composite (Metglas/PZT) to construct a tunable inductor for power electronics and RF integrated circuits. The results show an inductance tunable range up to 287% with improved quality factors more than 28 [5]. *Gao et al*. [6] have reported a power-efficient voltage tunable RF integrated magnetoelectric inductors with FeGaB/Al_2O_3 multilayer films, which showed a voltage tunable inductance of >100%. These voltage tunable RF multiferroic devices provide a compact and power efficient approach to frequency agile electronics with several orders of magnitude improved power efficiency compared to magnetic field or current tunable RF/microwave magnetic devices.

In this paper, we report on the first integrated non-reciprocal dual H- and E-Field tunable bandpass filter. With external in-plane magnetic fields from 100 to 400Oe, the central frequency was tuned from 3.78 to 5.27GHz, with an insertion loss of 1.73 to 3.42 dB and an isolation of more than 13 dB; by applying electric field from 0 kV/cm to 4 kV/cm, the BPF have a central frequency shift from 2.075 to 2.295.

II. Theory and Fabrication

A. MSW in Magnetized Ferrite

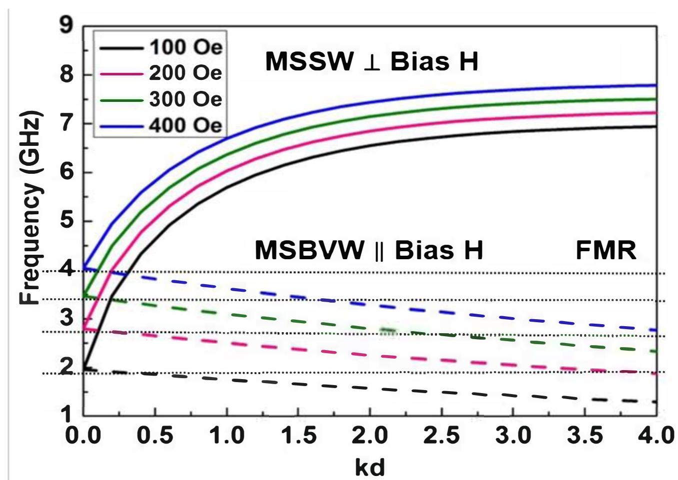

Fig. 1. Dispersion relation of MSW in infinite NiZn ferrite film, under 100 to 400Oe. The MSBVW part is for n=1 only.

By the magnetostatic approximation, the wave propagation in an infinite ferrite film follows the Walker's equation [7]:

$$(1+\chi)\left(k_x^2+k_y^2\right)+k_z^2=0$$

The dispersion relation of MSW under different dc bias field was calculated and plot as shown in Fig. 1. Under the bias condition $\overrightarrow{k} \perp \overrightarrow{H_{dc}}$, MSSW will be excited at the surface of the NiZn ferrite film [8]. Magnetic potential has a maximum at the surfaces and decays inside the slab with only one mode exists in the ferrite which starts upon the FMR frequency, given as:

$$e^{-2kd}=\frac{(\chi+2)^2-\kappa^2}{\chi^2-\kappa^2}$$

where k is the wave number and d is the film thickness.

Under the bias condition $\overrightarrow{k} \parallel \overrightarrow{H_{dc}}$, magnetostatic back volume wave (MSBVW) will be excited inside the NiZn ferrite film [8]. The magnetic potential has sinusoidal distribution and the back volume wave consists of multi-modes with the same cutoff frequencies given by:

$$tan\left(\frac{k_y d}{2\sqrt{-(1+\chi)}} - \frac{(n-1)\pi}{2}\right) = \sqrt{-(1+\chi)},\ n = 1,2,3 \ldots$$

MSBVW suffers from ripples due to the multi-resonance modes, while MSSW usually have a better resolution due to its single resonance.

B. Non-reciprocity Modeling

To diminish the splitting modes and achieve the non-reciprocity characteristics, the NiZn ferrite film was rotated ideally by 45 degree, as shown in Fig. 2(a). Suppose the bias magnetic field is applied in-plane and perpendicular to the MSSW. The reflection will propagate parallel to the bias field, which is operating in the stop-band of MSBVW, the reflected wave will decay fast and the energy dissipates along this path, and the standing-wave resonances will be diminished.

The radiation resistance per unit length for surface waves traveling in the (v=±1) direction can be written as [9]:

$$r_r^v = \frac{\mu_0 \omega}{2kd}\left[\frac{1+\chi}{(1+v\kappa)^2-(1+\chi)^2}\right]\left|\frac{F}{I}\right|^2$$
$$F = Ie^{-k_m s} J_0\left(\frac{k_m w}{2}\right)$$

where F indicates array factor for the current flowing on microstrip transducer, and J_0 is the Bessel function of zeroth-order, Fig. 2(b) shows the calculated radiation resistance under bias field of 400Oe. Due to the non-reciprocal field displacement, radiation resistance is different between MSSW propagating on forward and backward directions. We can assume more isolation and difference when we apply more bias field.

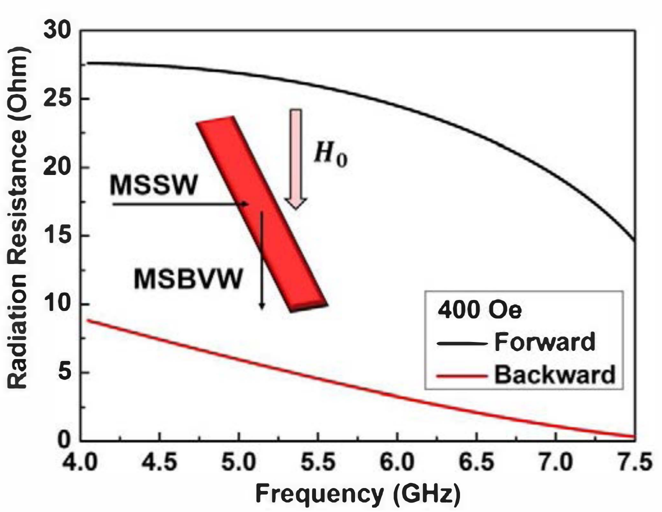

Fig. 2. Schematic of MSW propagation in a NiZn ferrite film with a rotate edge and calculated radiation resistances of forward and backward direction under 400Oe (b).

C. Magnetoelectric coupling

The changes of magnetic anisotropy can be approximated by using the inverse magnetoelastic relations. The PMN-PT slab will shrink in plane due to its negative piezoelectric coefficient d_{31} when a positive E-field is applied along the poling direction. The total effective anisotropy fields in the NiZn ferrite film can be expressed as [10]:

$$H_{eff} = H_a + H_{ME} = H_a + \frac{3\lambda_s \sigma}{M_s} = H_a + \frac{3\lambda_s Y d_{31} E}{M_s}$$

where H_a is the intrinsic in-plane anisotropy field of the ferrite film, H_{ME} is the E-field induced magnetic anisotropy field, M_s is the saturation magnetization, Y is the Young's modulus, and λ_s is the saturation magnetostriction constant of NiZn ferrite, which is ~ 20 ppm.

D. Fabrication Process

Fig. 3 shows the Optical photo (a) and the fabrication structure (b) of the integrated band-pass filter. The dimension of the filter is 1.35mm × 1mm. The NiZn feritte slab deposited via a low-temperature, low cost, and fast deposition spin sprayed process has the thickness of 2 microns. DRIE technique was used to remove Si substrate on the back side and the filters were bonded with ethyl cyanoacrylate glue to a 0.3mm thick ferroelectric (011) cut lead magnesium niobate - lead titanate PMN-PT slab that was poled along its thickness direction.

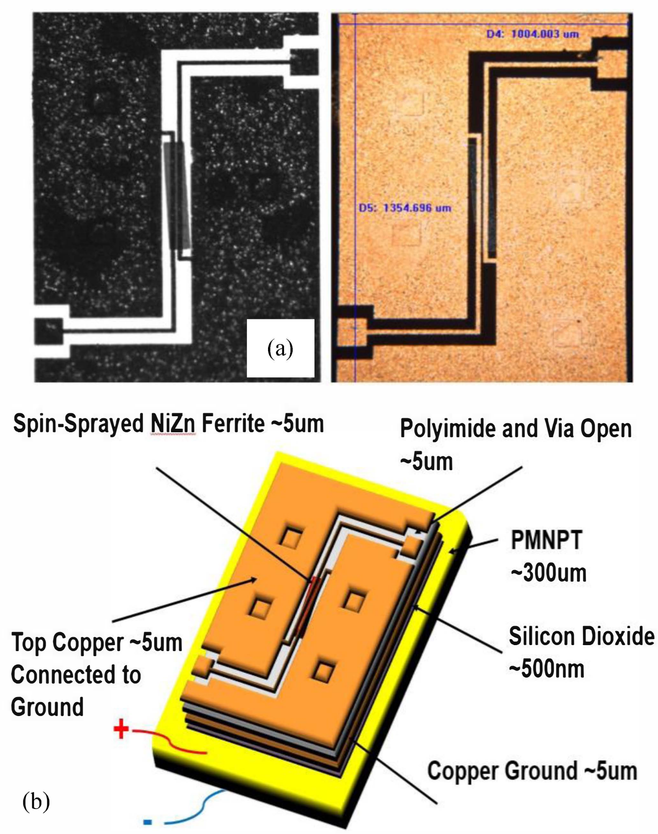

Fig. 3. Optical photo (a) and the fabrication structure (b) of the integrated bandpass filter.

III. RESULTS AND DISCUSSION

A. Simulation

The proposed transducers were simulated with Ansoft High Frequency Structure Simulator (HFSS) 14 and then fabricated and measured via a vector network analyzer (Agilent PNA E8364A). Fig. 4 shows the simulated S21 and S12 of the designed BPF. From the result we can expect to have center frequency tunability of 500MHz/100Oe with an insertion loss of 2.91 to 3.8dB. The maximum isolation could be found about 5.03dB with 400Oe dc bias field.

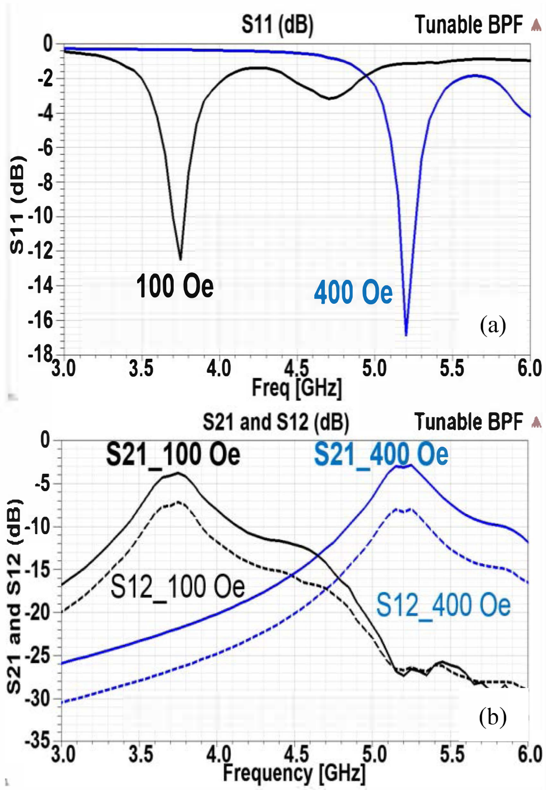

Fig. 4. Simulated results of BPF with a rotated NiZn ferrite resonator for S11 (a) S21 and S12 (b).

B. H-Field measurements

Fig. 5 shows the measured S-parameters of the designed BPF by applying dc bias field. The resonant frequencies and can be tuned by dc magnetic fields. Furthermore, non-reciprocal performance was observed with isolation over 13 dB between two transmission directions within the filter turning range from 3.78 to 5.27 GHz follow the Kittel's equation. Frequency tunability of 500MHz/100Oe is achieved with an insertion loss of 1.73 to 3.42 dB. The reflection coefficients S11 and S22 are less than 20 dB. This indicates that most of the energy dissipates in the NiZn ferrite film, instead of reflecting back at the ports when fed at port 2. The maximum isolation is 15.8B under 400Oe dc bias field at 5.35GHz. Fig. 6 shows the maximum isolation of 15.8B with 400Oe dc bias field at 5.35GHz. This isolation performance (difference between S21 and S12) is much better than the simulation result (5.03dB).

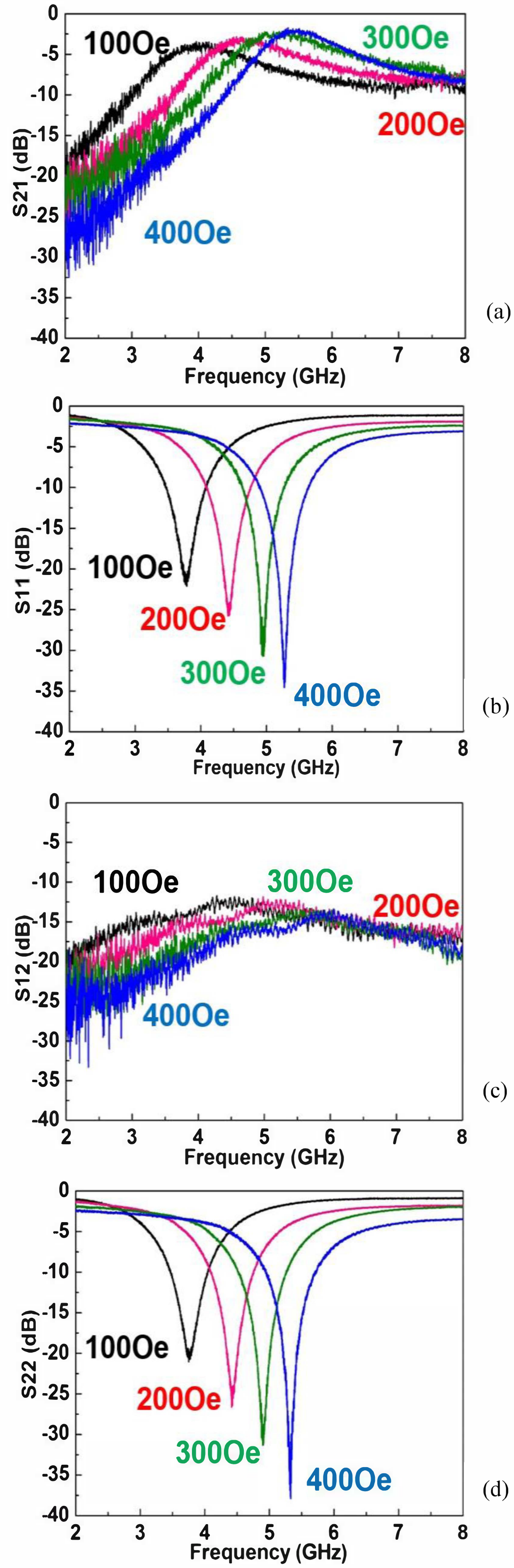

Fig. 5. Measured S-parameters of BPF with H-field tuning. S21 (a), S11 (b), S12 (c), and S22 (d)

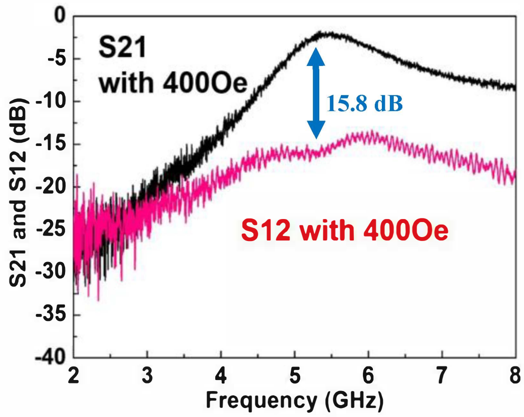

Fig. 6. The maximum isolation of 15.8B with 400Oe dc bias field at 5.35GHz.

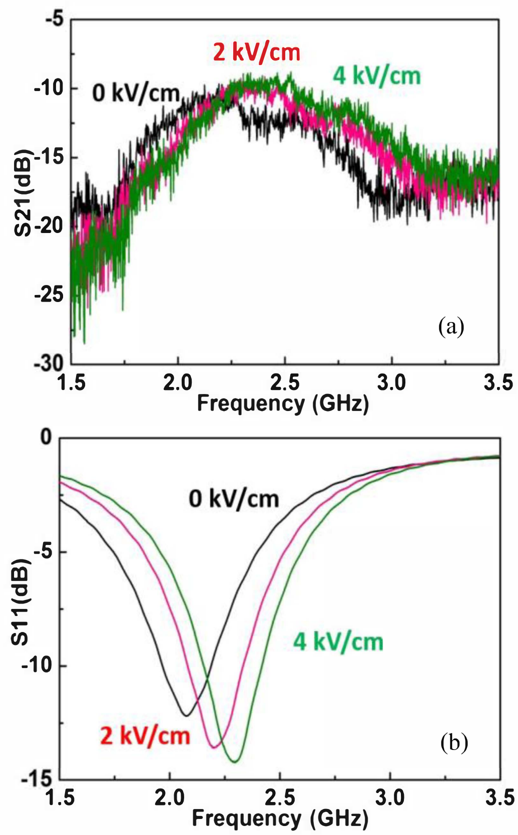

Fig. 7. Measured S21 (a), S11 (b) of BPF with E-field tuning after DRIE and attaching on the PMN-PT slab

C. E-Field measurements

Fig. 7 shows the measured S11 and S21 of the designed BPF after attaching on the PMN-PT slab. By applying Electric field, it performed a voltage tunable behavior, and the central frequency of the filter can be tuned from 2.075 to 2.295 GHz. Tunability of 55MHz/1(kV/cm) is achieved. The insertion loss is large comparing with the loss tuning by the H- field. We suspect that the reason is because that the strong DRIE process might cause oxidation of the copper, deformation of the structure and degradation of the magnetic material. However, it is still exciting in realizing power-efficiency voltage tunability for integrated RF devices.

IV. Conclusion

In summary, the first integrated tunable band-pass filter with ultra-wideband isolation is presented, fabricated, and tested, which is based on an inverted-S-shaped coupling structure loaded with a rotated NiZn ferrite film. MSSW propagation in the ferrite film leads to nonreciprocal performance. The tunable resonant frequency of 3.78 to 5.27 GHz was obtained for the BPF with a magnetic bias field of 100 to 400Oe applied perpendicular to the feed line. At the same time, the BPF acts as a UWB isolator with more than 13dB isolation at the pass-band with insertion loss of 1.73 to 3.42dB. With attaching the BPF on a PMN-PT slab, which performed a voltage tunable behavior, the central frequency of the filter can be tuned from 2.075 to 2.295 GHz. Frequency tunabilities of 500MHz/100Oe and 55MHz/1(kV/cm) are achieved. This design with dual functionality of integrated tunable band-pass filters and an UWB isolator will definitely be the future highlight in RF and microwave system.

References

[1] S. M. Hanna and S. Zeroug, “Single and coupled MSW resonators for microwave channelizers,” IEEE Trans. Magn., vol. 24, no. 6, pp. 2808–2810, Nov. 1988.

[2] W. S. Ishak and K. W. Chang, “Tunable microwave resonators using magnetostatic wave in YIG films,” IEEE Trans. Microw. Theory Tech., vol. 34, no. 12, pp. 1383–1393, Dec. 1986.

[3] J. D. Adam and S. N. Stitzer, “MSW frequency selective limiters at UHF,” *IEEE Trans. Magn.*, vol. 40, no. 4, pp. 2844–2846, Jul. 2004.

[4] Jing Wu, Xi Yang, Shawn Beguhn, Jing Lou and Nian X. Sun, “Nonreciprocal Tunable Low-Loss Bandpass Filters With Ultra-Wideband Isolation Based on Magnetostatic Surface Wave,” *IEEE Trans. Microwave Theory & Tech.,* vol. 60, no. 12, December 2012

[5] H. Lin, J. Lou, Y. Gao, Y. Hasegawa, M. Liu, B. Howe, J.G. Jones, G.J. Brown, and N. X. Sun, “Voltage Tunable Magnetoelectric Inductors with Improved Operational Frequency and Quality Factor for Power Electronics,” *IEEE Trans. Magn.* 51, 4002705, 2015

[6] Y. Gao, S. Zare, X. Yang, T. X. Nan, Z. Y. Zhou, M. Onabajo, M. Liu, A. Aronow, K. Mahalingam, B. M. Howe, G. J. Brown, and N. X. Sun, , “Significantly Enhanced Inductance and Quality Factor of GHz Integrated Magnetic Solenoid Inductors With FeGaB/Al_2O_3 Multilayer Films,” *IEEE Trans. Electron Devices* vol. 61*,* no. 5, May 2014

[7] E. Schlomann, “Microwave behavior of partially magnetized ferrites,” *J. Appl. Phys*., vol. 41, pp. 1350–1350, March. 1970

[8] D. Stencil, “Theory of Magnetostatic Waves,” *Berlin, Germany: Springer-Verlag, 1993.*

[9] J. D. Adam, “AN MSW tunable bandpass filter,” *IEEE Ultrason. Symp*., pp. 157–162, 1985

[10] J. Lou, D. Reed, M. Liu, and N. X. Sun, "Electrostatically tunable magnetoelectric inductors with large inductance tunability," *Appl. Phys. Lett.*, vol. 94, 112508, 2009